Chapter 5

Real-time Validation of a Hierarchical Coordinated Voltage Control Approach in high PV Penetrated Distribution System

5.1 Introduction

High penetration of photovoltaic (PV) generation in distribution system exacerbates the over voltage issue and violation of thermal limit of distribution lines. Further, this increased penetration leads to negative impact on system losses. In order to overcome above mentioned problems, an Hierarchical Coordinated Voltage Control Approach has been proposed in this chapter to reduce the energy demand as well as to eliminate the voltage violations in distribution system considering impact of advanced flexible power electronic devices such as PV and soft open point (SOP) smart inverter. To validate the developed approach, a real time co-simulation framework using real time digital simulator (RTDS) and MATLAB interface have been built.

5.2 Proposed Hierarchical Coordinated Voltage Control Approach

In this chapter, an hierarchical coordinated voltage control approach has been proposed to reduce the energy demand as well as to eliminate the voltage violations in distribution system as shown in Fig. 5.1

The proposed approach includes centralised control stage as well as local control stage. In

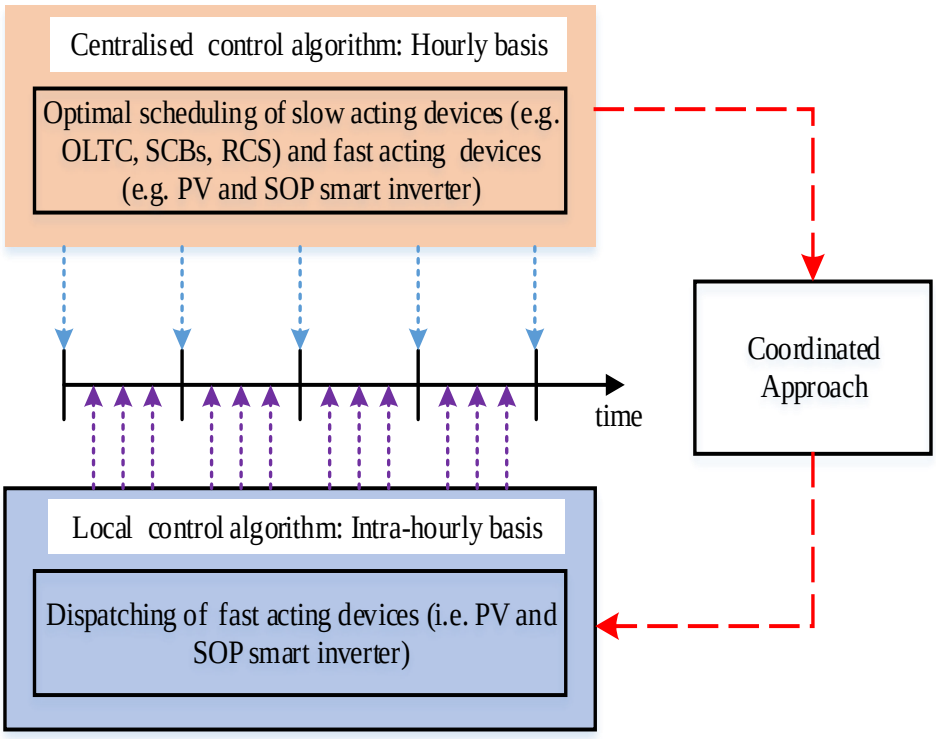

Figure 5.1: Implementation of proposed approach

the centralised control stage, scheduling of traditional devices (i.e. RCS, OLTC, SCBs) and advanced devices (i.e. PV and SOP smart inverter) has been determined under hourly/intra hour time scale with the objective of minimization of energy demand taking account of uncertainties of PV and load. While, in the local control stage, dispatch of advanced devices has been determined based on droop characteristics of smart inverters with the objective of mitigation of voltage violation in real time. For coordination purposes, the local control algorithm receives the obtained day ahead/intraday scheduled settings of PV and SOP smart inverter from centralised control algorithm. Further, correction in dispatch of PV and SOP smart inverter has been performed based on droop

characteristics of smart inverters in real time.

5.3 Problem formulation

The objective function is formulated as minimization of energy consumption and losses of the distribution system as given in equation (5.1)

$$OF1 = \sum_{t=1}^{T} \left[\overbrace{\sum_{i=1}^{nd} P_{i,cons.}^{t}}^{consumption} + \overbrace{\sum_{i=1}^{nd} P_{i,loss}^{t} + \sum_{i \in \Omega_{sop}} P_{i,sop}^{t,loss} + \sum_{i \in \Omega_{pv}} P_{i,pv}^{t,loss}}^{losses} \right] \tag{5.1}$$

In the equation (5.1), first terms represent the cost of energy consumption, second terms represents the energy losses in the network, PV smart inverter and SOP respectively.

system and operational constraints

- Active and reactive power balance constraints

$$P_{grid}^{t} - P_{i,cons}^{t} + P_{i,pv}^{t} + P_{i,sop}^{t} = \sum_{i=1}^{nd} V_i^t V_j^t \left[G_{ij}^t \cos(\delta_i^t - \delta_j^t) + B_{ij} sin(\delta_i^t - \delta_j^t) \right] \tag{5.2}$$

$$Q_{grid}^{t} - Q_{i,cons}^{t} + Q_{i,cap}^{t} + Q_{i,pv}^{t} + Q_{i,sop}^{t} = \sum_{i=1}^{nd} V_i^t V_j^t \left[G_{ij}^t sin(\delta_i^t - \delta_j^t) - B_{ij} cos(\delta_i^t - \delta_j^t) \right] \tag{5.3}$$

- Voltage dependent loads

$$P_{i,cons}^{t} = P_{i,cons}^{n,t} \left(\frac{V_i^t}{V_i^{n,t}} \right)^{k_i^p} \tag{5.4}$$

$$Q_{i,cons}^{t} = Q_{i,cons}^{n,t} \left(\frac{V_i^t}{V_i^{n,t}} \right)^{k_i^q} \tag{5.5}$$

- Bus voltage magnitude limits

$$V_{\min} \leq V_i^t \leq V_{\max} \tag{5.6}$$

- Tap settings of OLTC Transformer

$$V^t = 1 + tap^t \frac{\Delta V_{step}}{100} \tag{5.7}$$

here $tap^t \in \left\{ tap^{\min,t}, ..., -1, 0, 1, ...tap^{\max,t} \right\}$

- Shunt capacitor banks (SCBs) settings

$$Q_i^{cap,t} = st_i^t \Delta q_i^{cap}; i \in \Omega_{cap} \tag{5.8}$$

here $st_i^t \in \{0, 1, ...st_i^{\max}\}$

- PV smart inverter (PVSI) constraint

$$Q_{i,inv}^{\max,t} = \sqrt{\left(S_{i,pv}^{\max}\right)^2 - \left(P_{i,pv}^t\right)^2} \tag{5.9}$$

$$-Q_{i,inv}^{\max,t} \leq Q_{i,inv}^t \leq Q_{i,inv}^{\max,t} \tag{5.10}$$

$$P_{i,pv}^{t,loss} = \left(1 - \eta^{inv}\right) \sqrt{\left(P_{i,pv}^t\right)^2 + \left(Q_{i,pv}^t\right)^2} \tag{5.11}$$

$$P_{i,pv}^t = P_{i,pv}^{t,actual} - P_{i,pv}^{t,loss} \tag{5.12}$$

- Branch current limit

$$I_m^t \leq I_m^{\max} \tag{5.13}$$

- Radial structure constraint [126]

$$rank(\text{BBIM}) = nbr \tag{5.14}$$

- SOP active power constraints

$$P_{i,sop}^t + P_{j,sop}^t + P_{i,sop}^{t,loss} + P_{j,sop}^{t,loss} = 0 \tag{5.15}$$

$$P_{i,sop}^{t,loss} = A_{i,sop} \sqrt{\left(P_{i,sop}^t\right)^2 + \left(Q_{i,sop}^t\right)^2} \tag{5.16}$$

$$P_{j,sop}^{t,loss} = A_{j,sop} \sqrt{\left(P_{j,sop}^t\right)^2 + \left(Q_{j,sop}^t\right)^2} \tag{5.17}$$

- SOP reactive power constraints

$$Q_{i,sop}^{\min} \leq Q_{i,sop}^t \leq Q_{i,sop}^{\max} \tag{5.18}$$

$$Q_{j,sop}^{\min} \leq Q_{j,sop}^t \leq Q_{j,sop}^{\max} \tag{5.19}$$

- SOP capacity constraints

$$\sqrt{\left(P_{i,sop}^t\right)^2 + \left(Q_{i,sop}^t\right)^2} \leq S_{i,sop} \tag{5.20}$$

$$\sqrt{\left(P_{j,sop}^t\right)^2 + \left(Q_{j,sop}^t\right)^2} \leq S_{j,sop} \tag{5.21}$$

5.4 Implementation of Proposed Hierarchical Coordinated Voltage Control Approach in Real-Time

Fig.5.2 depicts complete implementation of proposed approach. For uncertainty modeling, scenario based technique has been employed. Here, the standard deviation of the forecasted PV output and load are taken as ± 15% and ± 10% of their mean value respectively for each hour. A Gaussian distribution [32] have been employed to simulate the PV output and the load demand, respectively. Further, Monte Carlo simulation has been performed with 500 scenarios. In order to reduce the computational burden, scenarios have been reducing to 15 scenarios by using k-means clustering [33].

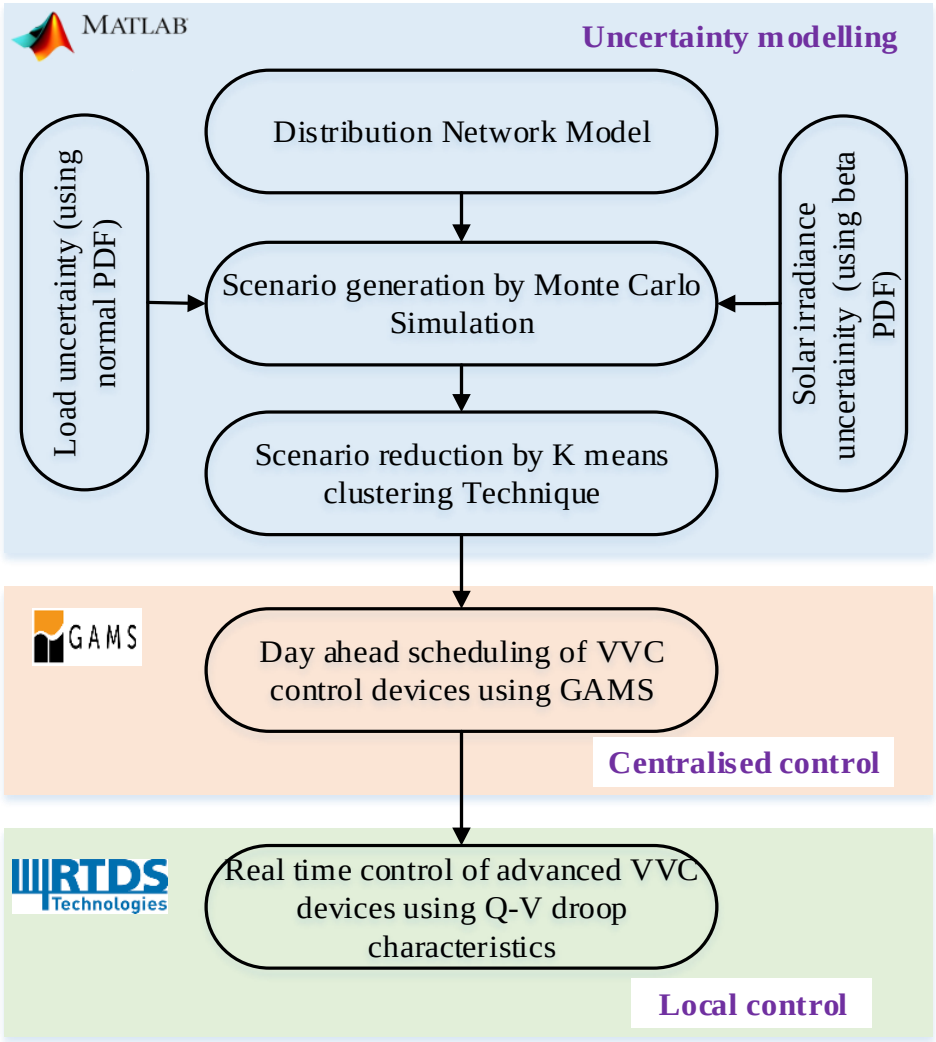

Figure 5.2: Implementation of proposed approach

As said earlier section 3,the optimal scheduling of remote-controlled switches, tradi-

tional and advanced VVC devices have been determined in centralised control algorithm on hourly/intra hourly basis considering uncertainties in PV generation and load. In this chapter, Discrete and continuous optimizer (DICOPT) solver of general algebraic modeling system (GAMS) platform [23] has been adopted to determine the optimal scheduling in centralised control algorithm. In DICOPT solver, a MINLP problem has been solved by a series of NLP (nonlinear programming) and MIP (mixed integer programming) sub problems. However, voltage violations may occurs within short time due to various reasons such as sudden variation of generation/load. In order to resolve this issue, local control algorithm has been performed in real time, based on the obtained scheduling of advanced VVC device.

The proposed local control strategy is based on Q-V droop characteristics, which is shown in Fig. 5.4. It is piecewise linear to the voltage and having the four points (A_1, A_2, A_3 and A_4). Before point A_1 , PV/SOP inverter can inject the available maximum reactive power to the point of connection (POC). From point A1 to A2, inverter can inject the additional reactive power to the POC. The range between point A_2 and A_3 defined as dead band (DB) range where SOP inverter neither injects nor absorbs reactive power. From point A_3 to A_4, inverter absorbs additional reactive power from the POC. After point A_4, SOP inverter absorbs the available maximum reactive power from the POC. The compensated reactive power ($Q^t_{i,pv/sop}$) at any instant, t is determined using (23).

$$Q^t_{i,pv/sop} = \begin{cases} Q^{\max}_{i,pv/sop} & V^t_i < V^{A_1}_1 \\ \frac{V^t_i - V^{A_2}_2}{V^{A_1}_1 - V^{A_2}_2}\left(Q^{\max}_{i,pv/sop}\right) & V^{A_1}_1 \leq V^t_i < V^{A_2}_2 \\ 0 & V^{A_2}_2 \leq V^t_i \leq V^{A_3}_3 \\ -\frac{V^t_i - V^{A_3}_3}{V^{A_4}_4 - V^{A_3}_3}\left(Q^{\max}_{i,pv/sop}\right) & V^{A_3}_3 < V^t_i \leq V^{A_4}_4 \\ -Q^{\max}_{i,pv/sop} & V^t_i > V^{A_4}_4 \end{cases} \tag{5.22}$$

5.5 Simulation results and discussions

The 33 bus distribution system has been chosen for the case study. The detailed line data and load data has been taken from [131]. The original system does not have any OLTC, SCBs and TVVD loads. Modifications in the original test system has been done to accommodate these devices explained as under.

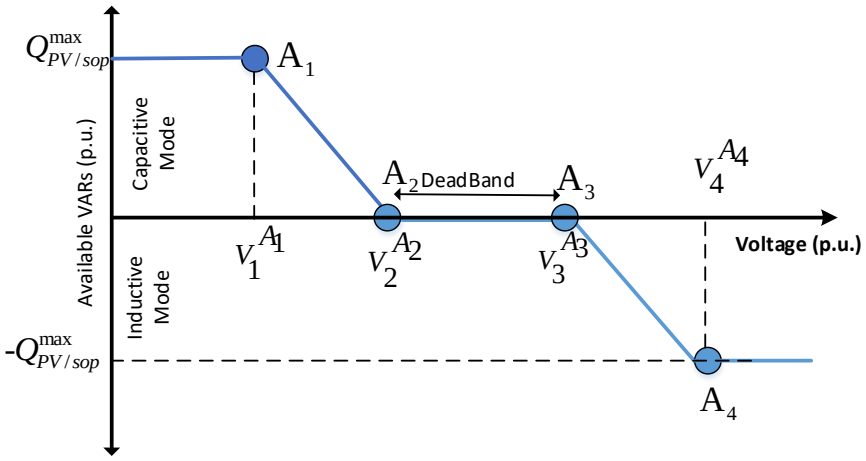

Figure 5.3: Droop characteristics of PV/SOP

5.5.1 Modified 33 bus system

In modified 33 bus system, it is assumed that OLTC transformer is connected between substation and node 1 and four SCBs are installed at buses 3, 6 , 11 and 23 respectively as shown in Fig. 5.4. The OLTC transformer can vary the substation secondary side voltage in the range of ±5% with 16 tap positions (-8,-7,,-1,0,1,2,,7,8), Change in each step would be 0.625%. It is assumed that the lower and upper permissible voltage limit are 0.95 pu to 1.05 pu respectively. Each SCBs can vary from 0 to 300 kVAR. Active (k_p) and reactive (k_q) power exponents of different types of customers such as industrial, residential and commercial are taken from ref. [120]. The SOP is installed between node 25 and 29. The capacity of SOP has been taken as 500 kVA. The lower and upper limit of reactive power has been considered as −300 kVAR and 300 kVAR. The loss coefficient of each VSC in SOP is taken as 0.02 [45]. Simulations have been carried out under MATLAB environment. PV based DGs are installed at buses 15,17 and 30 having capacity of 1200 kVA. Load profile and PV generation output over 24 hours have been plotted in Fig. 5.5. The parameters of GWO such as population size and number of iterations are taken as 50 and 100 respectively.

5.5.2 centralised control stage

In order to show the impact of proposed integrated operation on distribution system, five scenarios have been studied as under

- Scenario 1: No control

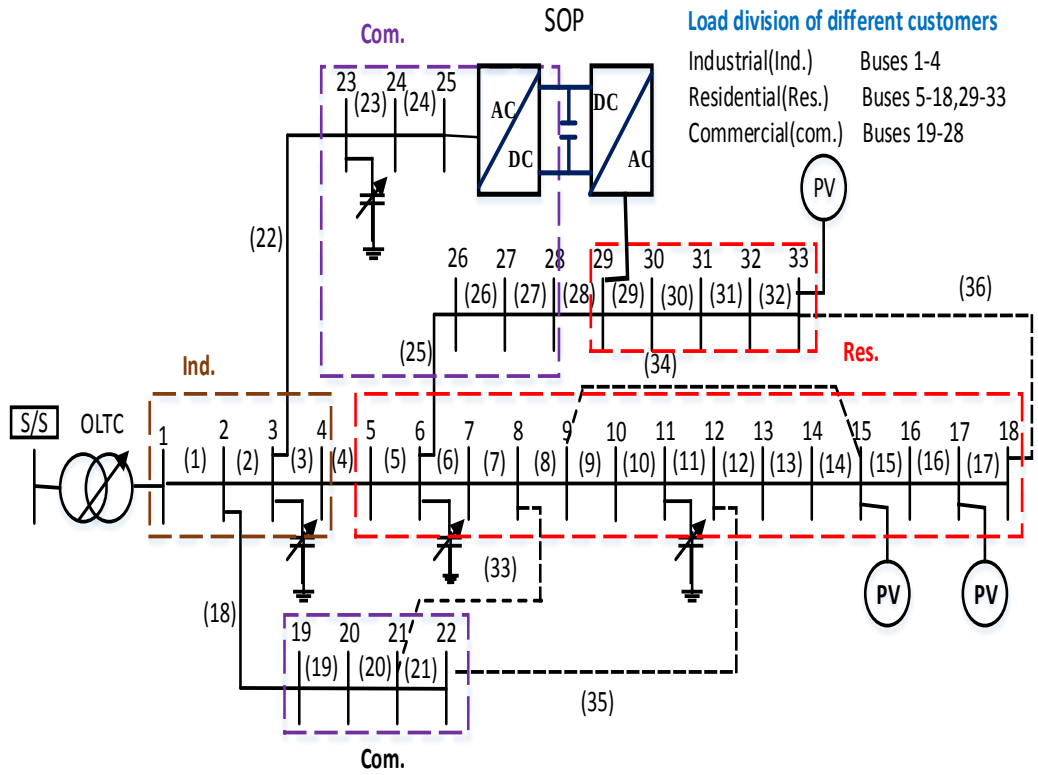

Figure 5.4: Modified 33 distribution system

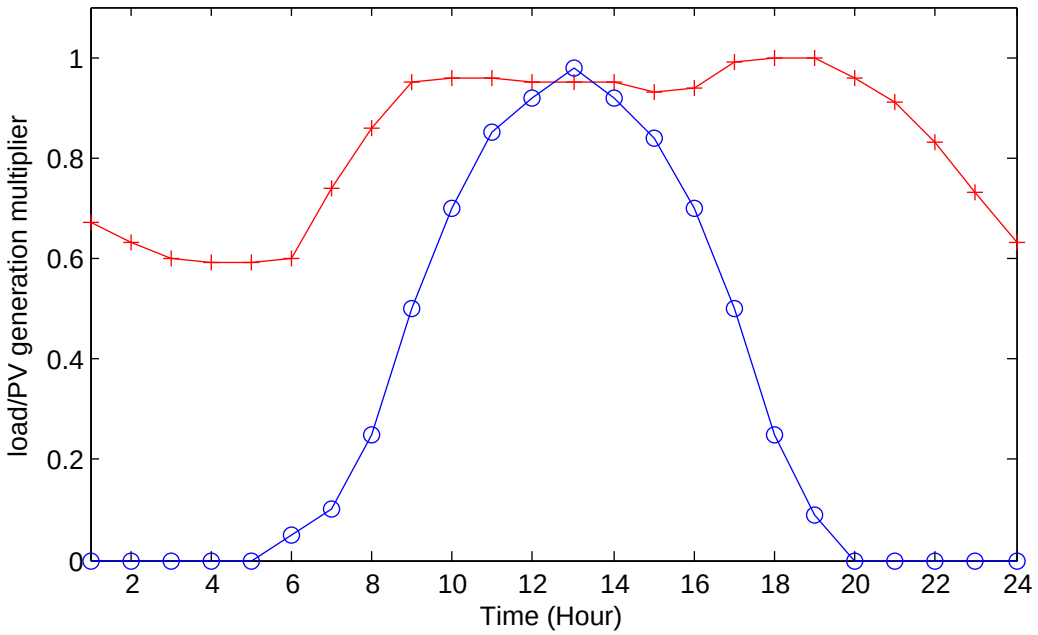

Figure 5.5: load and PV generation multiplier

- Scenario 2: optimal operation considering VVC devices and PVSI (method in [53])

- Scenario 3: optimal operation considering VVC devices, PVSI and DNR (method

in [127])

- Scenario 4: optimal operation considering VVC devices, PVSI and SOP (proposed method 1)
- Scenario 5: optimal operation considering VVC devices, PVSI, DNR and SOP (proposed method 2)

Table 5.1 shows the energy consumption, energy losses, minimum and maximum voltage of the system.

Table 5.1: simulation results under different scenarios

Scenarios		SC-1	SC-2	SC-3	SC-4	SC-5
$E_{cons.}$(MWh)		72.254	70.778	70.559	70.348	70.34
$\Delta E_{cons.}$(%)		—	2.042	2.345	2.637	2.648
$E_{loss.}$(MWh)	network	2.599	1.995	1.922	1.780	1.737
	SOP	—	—	—	0.105	0.087
	PVSI	—	0.204	0.208	0.183	0.181
	total	2.599	2.199	2.13	2.068	2.005
$\Delta E_{loss.}$(%)		—	15.39	18.04	20.43	22.854
Min. volt (pu)		0.92	0.95	0.95	0.95	0.95
Max. volt (pu)		1.064	1.043	1.047	1.042	1.033

5.5.2.1 Scenario-1

In this scenario, operation of VVC, DNR and SOP has not been considered. Status of SCBs in off state and set of opened RCS are 33, 34, 35, 36, 37. The energy consumption and energy network losses of the system have been recorded as 72.254 MWh and 2.599 MWh respectively.

5.5.2.2 Scenario-2

In this scenario, optimal VVC operation has been conducted using traditional VVC devices (i.e. OLTC taps and SCBs) and PV smart inverter. Status of RCS same as scenario 1. The energy consumption and losses of the system has been reduced to 70.778 MWh

(i.e. 2.042% reduction compared to scenario 1), and 2.199 MWh (i.e. 15.39% reduction compared to scenario 1) respectively.

5.5.2.3 Scenario-3

In this scenario, optimal VVC operation has been conducted using traditional VVC devices, PV smart inverter and DNR. Obtained optimal opened RCS has been shown in Table 5.2. The energy consumption and losses of the system has been reduced to 70.559 MWh (i.e. 2.345% reduction compared to scenario 1), and 2.13 MWh (i.e. 18.04% reduction compared to scenario 1) respectively.

5.5.2.4 Scenario-4

In this scenario, optimal VVC operation has been conducted using traditional VVC devices, PV smart inverter and SOP devices. Status of RCS same as scenario 1. Fig.5.6 and Fig.5.7 shows the active power transmission and reactive power compensation of SOP over a day respectively. The energy consumption and losses of the system has been reduced to 70.348 MWh (i.e. 2.637% reduction compared to scenario 1), and 2.068 MWh (i.e. 20.43% reduction compared to scenario 1) respectively.

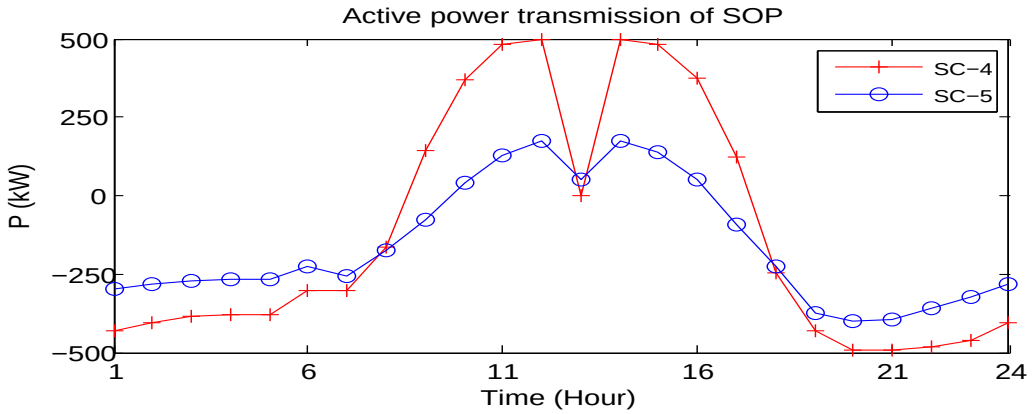

Figure 5.6: Active power transmission of SOP

5.5.2.5 Scenario-5

In this scenario, optimal VVC operation has been conducted using traditional VVC devices, PV smart inverter, DNR and SOP devices. Obtained optimal opened RCS has been

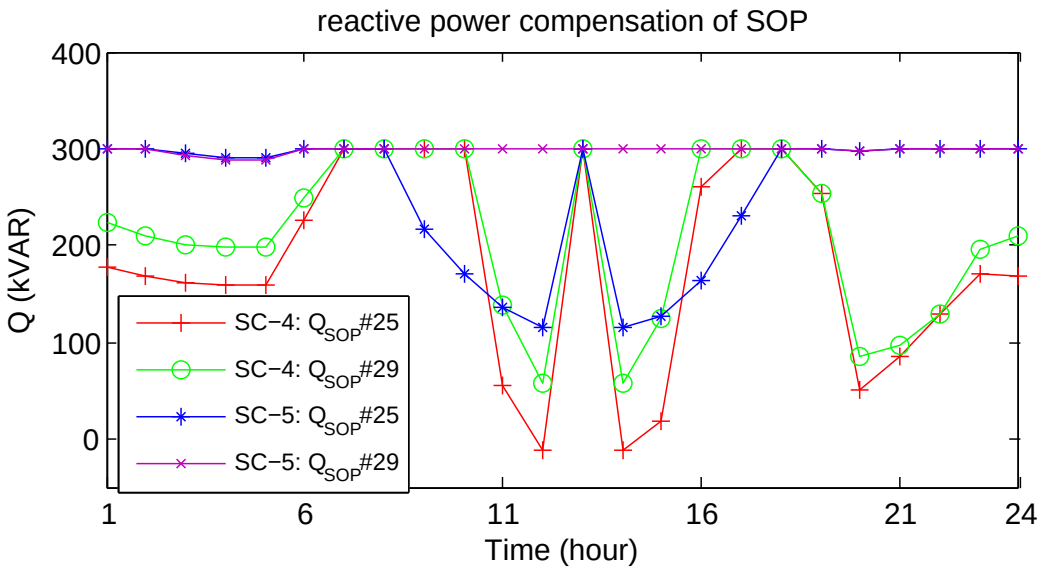

Figure 5.7: Reactive power compensation from SOP

shown in Table 5.2. Fig.5.6 and Fig.5.7 shows the active power transmission and reactive power compensation of SOP over a day respectively. The energy consumption and losses of the system has been reduced to 70.34 MWh (i.e. 2.648% reduction compared to scenario 1), and 2.005 MWh (i.e. 22.854% reduction compared to scenario 1) respectively.

Table 5.2: opened RCS under scenario 1 and 5

Hour duration	Scenario 3	Scenario 5
00:00 to 07:00	(7), (9), (14), (32), (37)	(6), (9), (13),(32), (37)
07:00 to 19:00	(7), (10), (14), (32), (37)	(7), (9), (13),(28), (37)
19:00 to 00:00	(7), (10), (14), (28), (32)	(6), (11), (14),(28), (37)

5.5.2.6 Voltage behavior of the system under different scenarios

Voltage behavior of the system at hour 13:00 (i.e. maximum PV output) and hour 19:00 (i.e. peak loading hour) have plotted in Fig.5.8 and Fig.5.9 respectively.

Due to high penetration of PV generation, voltage of the system violates the upper voltage limit as seen in Fig. 5.8 under scenario 1. Similarly, it can be observed from Fig. 5.9 at peak load hour, voltage of the system violates the lower voltage limit. With the implementation of proposed integrated scheme, both over/under voltage violations can be avoided as seen Fig. 5.8 and Fig. 5.9 respectively. Reduction of energy consumption

and losses up to 2.648 % and 22.854 % respectively can be achieved by proposed integrated operation scheme.

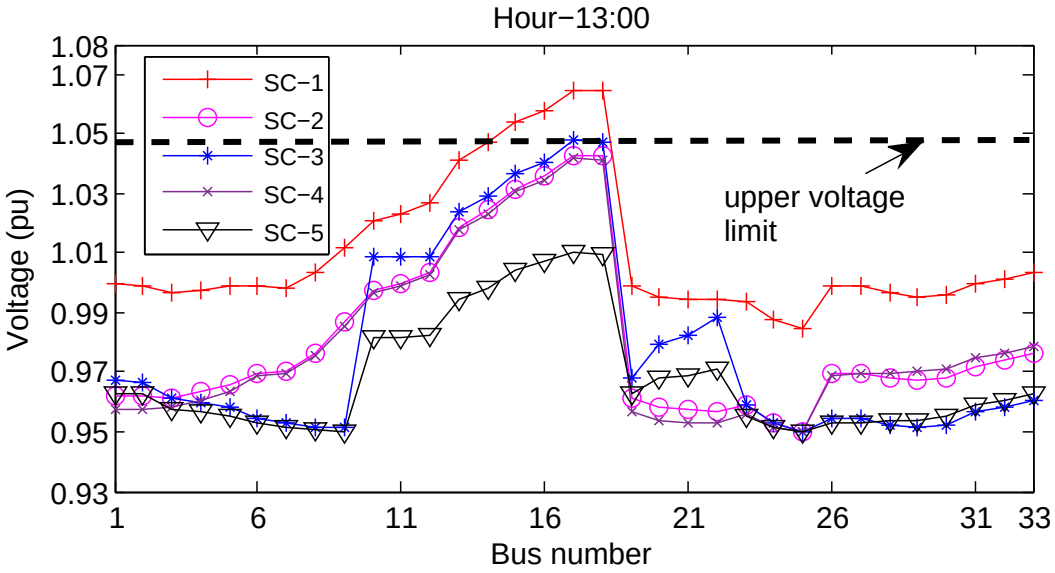

Figure 5.8: voltage behaviour at hour 13 under different scenarios

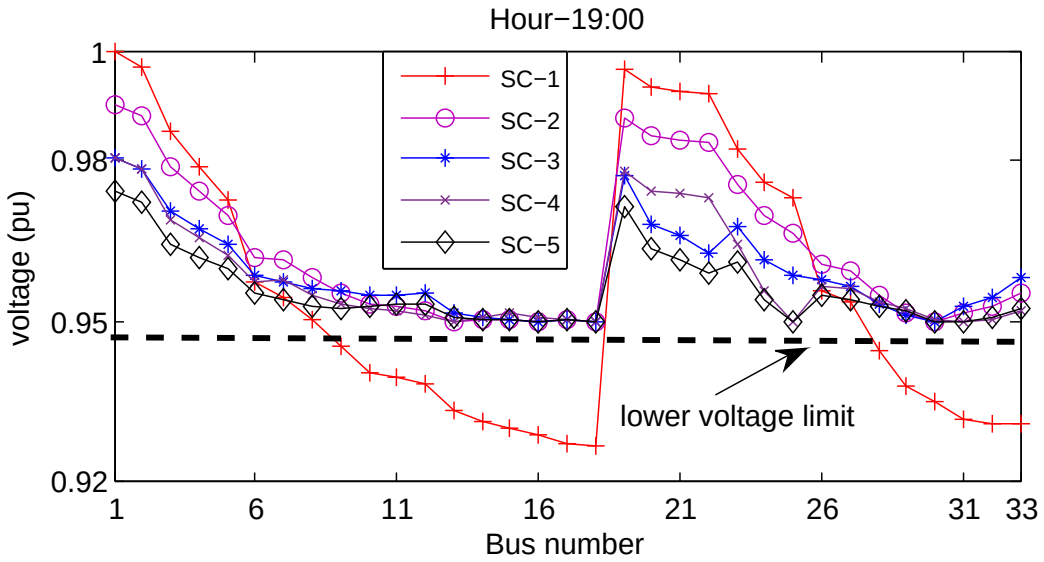

Figure 5.9: voltage behaviour at hour 19 different scenarios

5.5.3 Real time co-simulation platform

The proposed coordination control method has been implemented in real time using RTDS-MATLAB co−simulation platform. In this platform, the actual system and the control centre have been simulated by RSCAD and MATLAB-GAMS environment

Table 5.3: optimal scheduling of control devices obtained by centralised control stage at 14:00 hour

OLTC Tap position	SCBs step position	Opened RCS	Active/Reactive power from PV inverter (MW/ MVAR)	Active/Reactive power from SOP inverter (MW/ MVAR)	Voltagesat buses {15, 17, 33, 25, 29} in (pu
-6	{1,0,0,1}	(7), (9), (13), (28), (37)	P{0.95,0.95,0.95}; Q{-0.3,-0.039,0.11}	P{0.08,-0.08}; Q{0.1, 0.3}	{0.998,0.99, 0.955, 0.952, 0.951}

respectively. The GTNET-SKT (SocKeT) Protocol has been utilized to provide a real time communication link between the RTDS simulator and MATLAB-GAMS installed computer via Ethernet. Fig. 5.10 represents the pictorial view of co-simulation platform

5.5.3.1 Simulation procedure

The distribution system model as shown in figure 5 has been modelled and simulated in real time digital simulator (RTDS) through its software interface RSCAD (i.e. RTDS NovaCor, RSCAD 5.007). The simulation has been carried out in *Distribution Mode* with simulation time step (dt) of 150 micro-seconds. The modelling of PV and SOPs have been built using *Average Models* available in RSCAD library. The centralized control algorithm (coded in MATLAB-GAMS environment) executed in Computer I. Then, the control commands generated from MatLab-GAMS will be sent to RTDS through GTNET-SKT communication at hourly/intra hourly basis. The local control algorithm (coded in RSCAD environment) executed in Computer II, which performed in real time.

5.5.3.2 Validation of local control algorithm in real time

In order to validate the Q-V droop control of PV and SOP inverter in real time scale, the hour 14:00 have been taken, where optimal scheduling of control devices obtained by centralised control stage have been given in table 5.3. At hour 14:00, forecasted load and PV output about 0.93% of peak demand and 0.92% of the peak. In order to analyse the effect of cloud transients, it is assumed that the sudden fall of solar irradiance from 0.92 kW/m^2 to 0.5 kW/m^2 has been occurred on the PV system, corresponding PV active power output has been dropped. The following two cases has been studied to show the effectiveness of proposed local control algorithm under cloud transient condition.

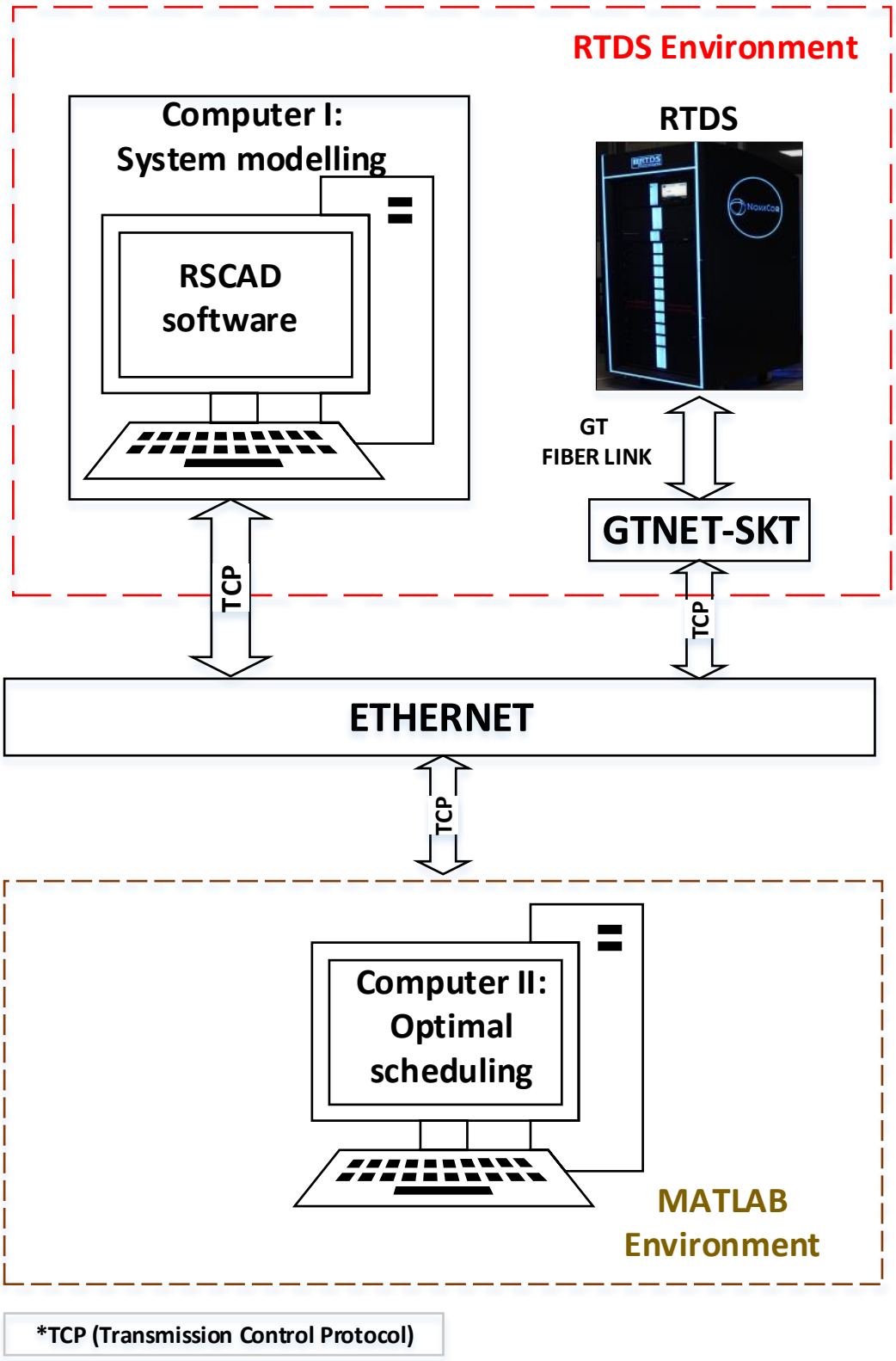

Figure 5.10: Structure of Real Time Co-simulation Platform

- Case 1: Without local control
- Case 2: With local control

From Fig. 5.11, it can be observed that the voltages at PV installed buses (i.e. bus 15, bus 17 and bus 33) and SOP connected buses (i.e. bus 25, bus 29) of the 33−bus distribution system have been violated the lower permissible limit (i.e. 0.95 pu) in case 1, due to cloud transient effect on PV generation output. where as, in case 2, the voltage violations at respective buses have been mitigated by reactive power support from the PV and SOP smart inverter as seen Fig. 5.12.

5.6 Conclusion

This chapter has presented a hierarchical coordinated voltage control approach for minimization of energy consumption, energy losses and mitigation of voltage violations. The simulated results reveal that significant amount of energy consumption and losses can be achieved with combined integrated operation. The over voltage problem during higher PV power injection and under voltage problem during peak load condition has also been rectified. Further reduction in energy consumption and losses can be achieved by PV and SOP smart inverter. The proposed local control algorithm can efficiently work even in sudden change in the PV power generation.

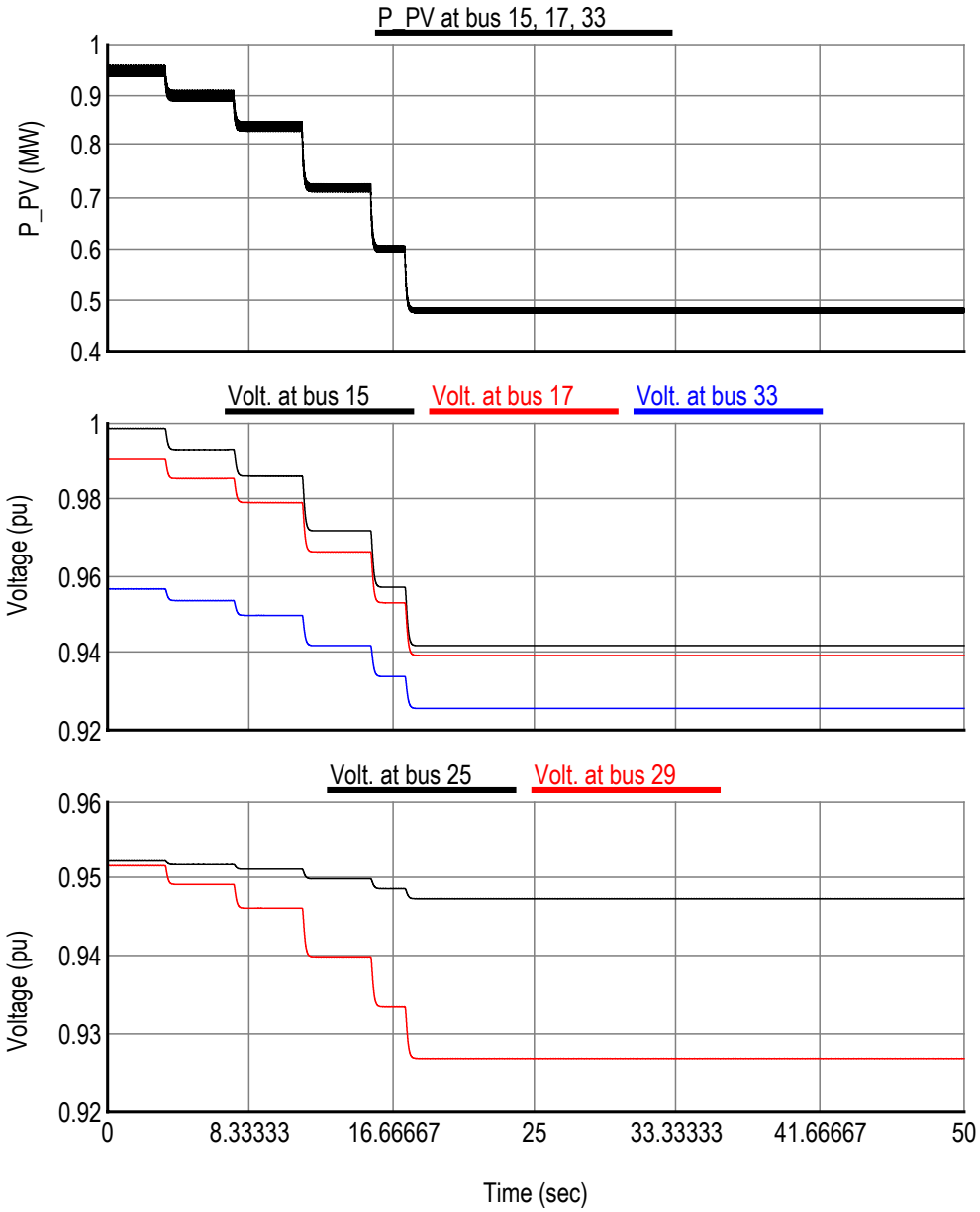

Figure 5.11: PV active power output and voltage behaviour in case 1 under cloud transient condition

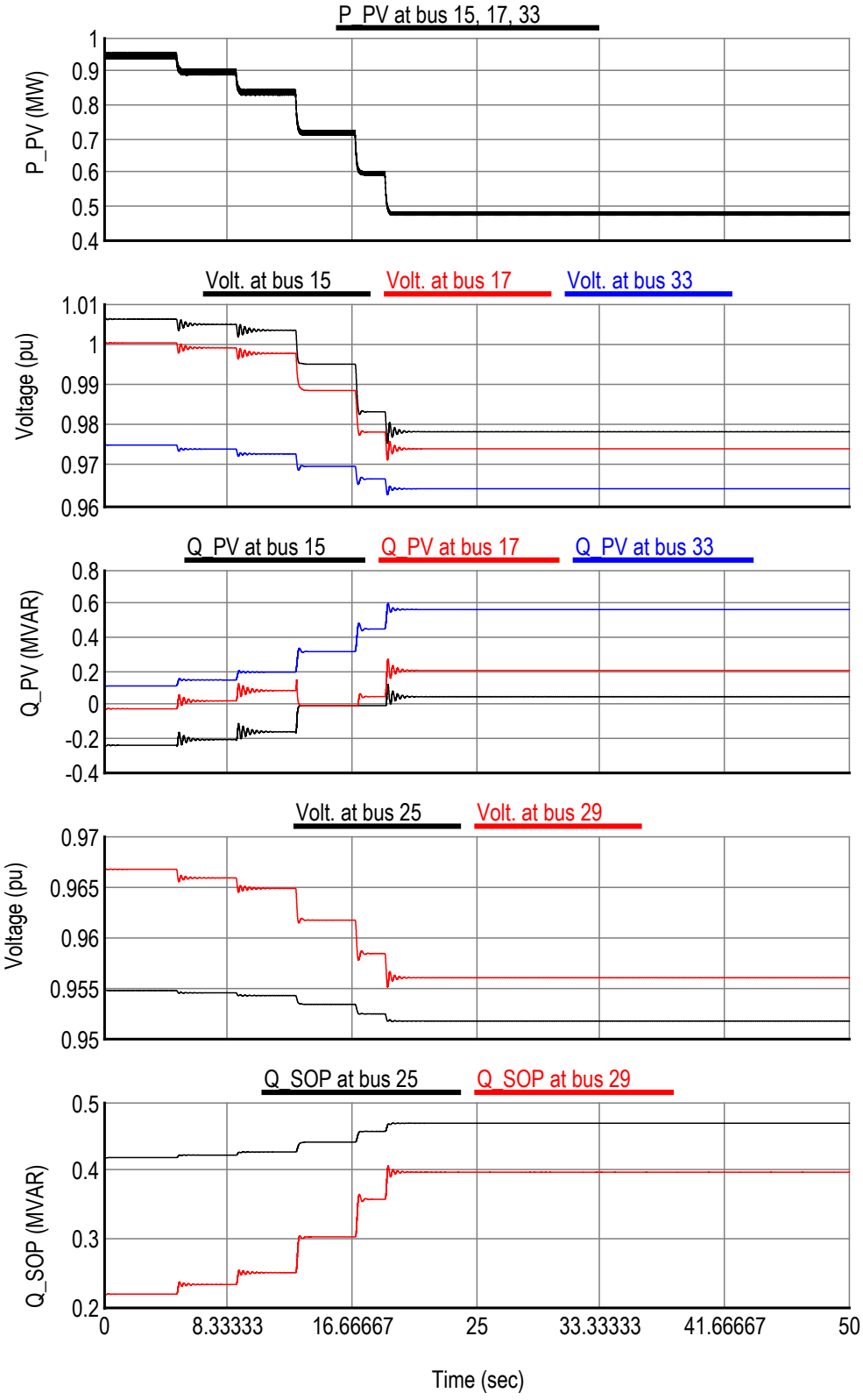

Figure 5.12: PV active power output, voltage behaviour and reactive power output of PV, SOP smart inverter in case 2 under cloud transient condition